Theoretical Development of an Orthotropic Elasto-Plastic Generalized Composite Material Model

Robert K. Goldberg and Kelly S. Carney
NASA Glenn Research Center, Cleveland OH
Paul Du Bois
George Mason University, Fairfax VA
Canio Hoffarth, Joseph Harrington and Subramaniam Rajan
Arizona State University, Tempe AZ
Gunther Blankenhorn
Livermore Software Technology Corporation, Livermore CA

Copyright by DYNAmore

Abstract

The need for accurate material models to simulate the deformation, damage and failure of polymer matrix composites is becoming critical as these materials are gaining increased usage in the aerospace and automotive industries. While there are several composite material models currently available within LS-DYNA®, there are several features that have been identified that could improve the predictive capability of a composite model. To address these needs, a combined plasticity and damage model suitable for use with both solid and shell elements is being developed and is being implemented into LS-DYNA as MAT_213. A key feature of the improved material model is the use of tabulated stress-strain data in a variety of coordinate directions to fully define the stress-strain response of the material. To date, the model development efforts have focused on creating the plasticity portion of the model. The Tsai-Wu composite failure model has been generalized and extended to a strain-hardening based orthotropic material model with a non-associative flow rule. The coefficients of the yield function, and the stresses to be used in both the yield function and the flow rule, are computed based on the input stress-strain curves using the effective plastic strain as the tracking variable. The coefficients in the flow rule are computed based on the obtained stress-strain data. The developed material model is suitable for implementation within LS-DYNA for use in analyzing the nonlinear response of polymer composites.

Introduction

As composite materials are gaining increasing use in aircraft components where impact tolerance is important (such as the turbine engine fan case), the need for accurate material models to simulate the deformation, damage and failure response of polymer matrix composites under impact conditions is becoming more critical. Within LS-DYNA® [1], there are several material models available for application to the analysis of composites. For example, the Chang-Chang failure model [2] is utilized in MAT_22 and MAT_54. In these models, combinations of ratios of stresses to failure strengths are utilized to predict fiber or matrix based failure. The response is assumed be linear elastic, with limited capability to simulate the nonlinear shear response. In MAT_22 the failure is assumed to be brittle, while in MAT_54 the composite elastic constants

are selectively reduced based on the failure mode, and a gradual unloading is permitted until ultimate element failure is reached. In MAT_58, a continuum damage model developed by Matzenmiller et al [3] is employed, where the initiation and accumulation of damage is assumed to be the primary driver of the nonlinearity in the composite response. The failure stresses and strains of the material in each of the coordinate directions are specified by the user, and the material stress-strain curves are approximated based on this data. The original version of the material model assumes a material response that is independent of strain rate. However, in MAT_158 a modified version of the model is employed which incorporates strain rate dependence into the material response [1]. A viscoelastic Prony series based on shear moduli is used to modify the computed stresses. The strain rate dependence in all of the coordinate directions is assumed to be identical. MAT_161 is an additional continuum damage mechanics model available within LS-DYNA [4]. A stress to strength ratio approach in a variety of coordinate directions is used to specify the beginning of either fiber or matrix based failure. Appropriate failure mode based damage functions are then used to compute the reduction in elastic moduli in each of the coordinate directions. In MAT_219, based on the CODAM model [5], a strain versus failure strain ratio based approach is used to predict the initiation of damage in a sublaminate of the composite. Separate damage accumulation and modulus reduction functions based on failure mode and coordinate direction are implemented in a continuum damage mechanics formulation. In MAT_221, damage accumulation functions based on current strains, damage initiation strains and failure strains are used to reduce the elastic moduli of the composite in each of the coordinate directions in a damage mechanics approach [1]. In MAT_261, which is based on a damage and failure model developed by Pinho et al [6,7], separate models for fiber tension failure, fiber kinking failure, matrix tensile failure and matrix compressive failure are developed, where different functional forms are used for each of the failure criteria (for example, the matrix compression failure criterion is based on an extension of the Mohr-Coulomb failure criterion). The various failure criteria are combined together using fracture mechanics concepts to develop a constitutive model. In MAT_262, based on a model developed by Camonho, et al [8,9], an energy approach is utilized to generate damage functions in various coordinate directions within the context of a continuum damage mechanics formulation.

While all of the material models discussed above have been utilized with some level of success in modeling the impact response of polymer composites, there are some areas where the predictive capability can be improved. In general, the existing models often require significant a priori knowledge of the damage and failure such that their use as predictive tools can be limited. While these models generally assume that the nonlinear response of the composite is due to either deformation mechanisms (plasticity) or damage mechanisms, an improved model should have the capability to simulate the actual material behavior in which the material nonlinearity is due to a combination of both deformation and damage mechanisms. The input to the current material models generally consists of point-wise properties that lead to curve fit approximations to the material stress-strain curves. This type of approach leads to either models with only a few parameters, which provide a crude approximation at best to the actual stress-strain curve, or to models with many parameters which require a large number of complex tests to characterize. An improved approach would be to use tabulated data from a well-defined set of experiments to accurately define the complete stress-strain response of the material. Furthermore, many of the existing models are only suitable for use with two-dimensional shell elements, which cannot capture the through-thickness response which might be significant in impact applications. Ideally, a fully three-dimensional formulation suitable for use with solid elements would be

Copyright by DYNAmore

available, along with the shell element formulation. In addition, incorporating the effects of strain rate is only possible in a few of the existing models, and in those models, the effects of strain rate on the material response are assumed to be the same in all of the material coordinate directions.

To begin to address these needs, a multi-institution consortium has been formed to develop and implement a new composite material model within LS-DYNA, which will be implemented as MAT_213. Currently, the primary focus of the effort has been on the development and testing of the orthotropic macroscopic three-dimensional plasticity model. As will be discussed in more detail in the following sections of this paper, the commonly used Tsai-Wu composite failure criterion [10] has been generalized and extended to a strain-hardening model with a non-associative flow rule. A similar approach has been used by Sun and Chen [11], in which a general quadratic plastic potential function was generalized into a plasticity model suitable for use with composites. The coefficients of the yield function for the new composite model are determined based on tabulated stress-strain curves in the various normal and shear directions, along with selected off-axis curves. The non-associative flow rule is used to compute the components of the plastic strain along with the effective plastic strain. The stresses that are used in the flow rule are computed based on the input tabulated stress-strain curves. Systematic procedures have been developed to compute the various coefficients in the yield function and the flow rule based on the tabulated input data. An important point to note is that the developed material law is not limited to the analysis of unidirectional plies alone. Alternatively, the material model is meant to be a fully generalized model suitable for use with any composite architecture (unidirectional, laminated or textile). In the following sections of this paper, a detailed derivation of the yield function and the flow law are presented. The procedures to be used to characterize the material constants in the yield function and the flow law are also discussed in detail. Details of the numerical implementation of the material model within LS-DYNA and descriptions of verification and validation studies that were conducted using the developed material model are available in a companion paper [12].

Material Law Derivation

A general quadratic three-dimensional orthotropic yield function based on the Tsai-Wu failure model is specified as follows, where 1-2-3 refer to the principal material directions.

$$f(\sigma) = a + \begin{pmatrix} F_1 & F_2 & F_3 & 0 & 0 & 0 \end{pmatrix} \begin{pmatrix} \sigma_{11} \\ \sigma_{22} \\ \sigma_{33} \\ \sigma_{12} \\ \sigma_{23} \\ \sigma_{31} \end{pmatrix} + \begin{pmatrix} \sigma_{11} & \sigma_{22} & \sigma_{33} & \sigma_{12} & \sigma_{23} & \sigma_{31} \end{pmatrix} \begin{pmatrix} F_{11} & F_{12} & F_{13} & 0 & 0 & 0 \\ F_{12} & F_{22} & F_{23} & 0 & 0 & 0 \\ F_{13} & F_{23} & F_{33} & 0 & 0 & 0 \\ 0 & 0 & 0 & F_{44} & 0 & 0 \\ 0 & 0 & 0 & 0 & F_{55} & 0 \\ 0 & 0 & 0 & 0 & 0 & F_{66} \end{pmatrix} \begin{pmatrix} \sigma_{11} \\ \sigma_{22} \\ \sigma_{33} \\ \sigma_{12} \\ \sigma_{23} \\ \sigma_{31} \end{pmatrix} \quad (1)$$

In the yield function, σ_{ij} represents the stresses and F_{ij} are coefficients that vary based on the current values of the yield stresses in the various coordinate directions. By allowing the coefficients to vary, the yield surface evolution and hardening in each of the material directions can be precisely defined. The values of the normal and shear coefficients can be determined by simplifying the yield function for the case of unidirectional tensile and compressive loading in each of the coordinate directions along with shear tests in each of the shear directions, with results as shown below.

Copyright by DYNAmore

$$a = -1$$

$$\begin{aligned} F_1 &= \frac{1}{\sigma_{11}^T} - \frac{1}{\sigma_{11}^C} \qquad F_{11} = \frac{1}{\sigma_{11}^T \sigma_{11}^C} \qquad F_{44} = \frac{1}{\sigma_{12}^2} \\ F_2 &= \frac{1}{\sigma_{22}^T} - \frac{1}{\sigma_{22}^C} \qquad F_{22} = \frac{1}{\sigma_{22}^T \sigma_{22}^C} \qquad F_{55} = \frac{1}{\sigma_{23}^2} \\ F_3 &= \frac{1}{\sigma_{33}^T} - \frac{1}{\sigma_{33}^C} \qquad F_{33} = \frac{1}{\sigma_{33}^T \sigma_{33}^C} \qquad F_{66} = \frac{1}{\sigma_{31}^2} \end{aligned} \tag{2}$$

In the above equation, the stresses are the current value of the yield stresses in the normal and shear directions (determined using procedures to be discussed below), where the superscript T represents the tensile yield stress, and the superscript C represents the absolute value of the compressive yield stress. To determine the values of the off-axis coefficients (which are required to capture the stress interaction effects), the results from 45° off-axis tests in the various coordinate directions can be used. For example, the stresses in the local material axis system resulting from a uniaxial tensile test of a [45°] composite (for a unidirectional composite), or any uniaxial tensile test conducted at 45° in the 1-2 plane from the longitudinal (1) material axis for a multi-ply laminated or textile composite, can be computed to be the following by the stress transformation equations [10].

$$\begin{aligned} \sigma_{11} &= 0.5\sigma^{45} \\ \sigma_{22} &= 0.5\sigma^{45} \\ \sigma_{12} &= -0.5\sigma^{45} \end{aligned} \tag{3}$$

In the above equation, σ^{45} is the structural level current uniaxial yield stress resulting from the off-axis tensile test, and the remaining stresses are the material axis system based stresses. By substituting this equation into Equation (1) and solving, the following expression can be obtained for the off-axis constant F_{12}

$$F_{12} = \frac{2}{\left(\sigma^{45}\right)^2} - \frac{F_1 + F_2}{\sigma^{45}} - \frac{1}{2}\left(F_{11} + F_{22} + F_{44}\right) \tag{4}$$

where all of the terms are as defined earlier. By using similar procedures involving 45° rotations in the 2-3 plane and the 1-3 plane, similar expressions for the constants F_{23} and F_{31} can be determined.

A non-associative flow rule is used to compute the evolution of the components of plastic strain. The plastic potential for the flow rule is as shown below

$$h = \sqrt{H_{11}\sigma_{11}^2 + H_{22}\sigma_{22}^2 + H_{33}\sigma_{33}^2 + 2H_{12}\sigma_{11}\sigma_{22} + 2H_{23}\sigma_{22}\sigma_{33} + 2H_{31}\sigma_{33}\sigma_{11} + H_{44}\sigma_{12}^2 + H_{55}\sigma_{23}^2 + H_{66}\sigma_{31}^2} \tag{5}$$

where σ_{ij} are the current values of the stresses and H_{ij} are independent coefficients, which are assumed to remain constant. Procedures for determining the values of the coefficients will be discussed later in this paper. The plastic potential function in Equation (5) is used as follows in a

Copyright by DYNAmore

flow law, where the usual normality hypothesis from classical plasticity [13] is assumed to apply and the variable λ is a scalar plastic multiplier.

$$\dot{\varepsilon}^p = \dot{\lambda}\frac{\partial h}{\partial \sigma}$$

$$\dot{\varepsilon}_{11}^p = \frac{\dot{\lambda}}{2h}\left(2H_{11}\sigma_{11} + 2H_{12}\sigma_{22} + 2H_{13}\sigma_{33}\right)$$

$$\dot{\varepsilon}_{22}^p = \frac{\dot{\lambda}}{2h}\left(2H_{12}\sigma_{11} + 2H_{22}\sigma_{22} + 2H_{23}\sigma_{33}\right)$$

$$\dot{\varepsilon}_{11}^p = \frac{\dot{\lambda}}{2h}\left(2H_{13}\sigma_{11} + 2H_{23}\sigma_{22} + 2H_{33}\sigma_{33}\right) \tag{6}$$

$$\dot{\varepsilon}_{12}^p = \frac{\dot{\lambda}}{2h}H_{44}\sigma_{12}$$

$$\dot{\varepsilon}_{23}^p = \frac{\dot{\lambda}}{2h}H_{55}\sigma_{23}$$

$$\dot{\varepsilon}_{12}^p = \frac{\dot{\lambda}}{2h}H_{66}\sigma_{31}$$

In the above equation, ε_{ij}^p are the components of plastic strain. For the shear components, tensorial, not engineering, strains are used. By examining ratios of the components of plastic strain, the normal and off-axis coefficients H_{ij} in the plastic potential function can be related to "plastic Poisson's ratios" as follows, which as will be shown later in this paper, is useful in developing procedures to characterize the values of the coefficients.

$$\sigma_{11} \neq 0 \qquad \sigma_{22} \neq 0 \qquad \sigma_{33} \neq 0$$

$$\nu_{12}^p = -\frac{\dot{\varepsilon}_{22}^p}{\dot{\varepsilon}_{11}^p} = -\frac{H_{12}}{H_{11}} \qquad \nu_{21}^p = -\frac{\dot{\varepsilon}_{11}^p}{\dot{\varepsilon}_{22}^p} = -\frac{H_{12}}{H_{22}} \qquad \nu_{32}^p = -\frac{\dot{\varepsilon}_{22}^p}{\dot{\varepsilon}_{33}^p} = -\frac{H_{23}}{H_{33}} \tag{7}$$

$$\nu_{13}^p = -\frac{\dot{\varepsilon}_{33}^p}{\dot{\varepsilon}_{11}^p} = -\frac{H_{13}}{H_{11}} \qquad \nu_{23}^p = -\frac{\dot{\varepsilon}_{33}^p}{\dot{\varepsilon}_{22}^p} = -\frac{H_{23}}{H_{22}} \qquad \nu_{31}^p = -\frac{\dot{\varepsilon}_{11}^p}{\dot{\varepsilon}_{33}^p} = -\frac{H_{13}}{H_{33}}$$

An important point to note is that while the yield function can accommodate differences between the tensile and compressive responses of the composite, the flow law, due to its lack of linear terms, cannot make such a distinction. However, introduction of a linear term would make the plastic Poisson's ratio, and thus the coefficients in the flow law, highly dependent on the stress which would most likely lead to erratic behavior of the model. Another consideration is that the coefficients of the flow law could be assumed to vary based on the current stress and strain state, but that would require developing evolution conditions on the flow law, which would be very difficult to determine based on experimental data.

Given the flow law, the principal of the equivalence of plastic work [13] can be used to determine expressions for the effective stress and effective plastic strain. By taking the vector product of the stress tensor and the effective plastic strain tensor, one ends up with the plastic potential function multiplied by the plastic multiplier λ. Since by the principal of the

Copyright © DYNAmore

equivalence of plastic work the vector product of the effective stress and the effective plastic strain must equal the product of the effective stress and the effective plastic strain, one can conclude that the plastic potential function h can be defined as the effective stress and the plastic multiplier λ can be defined as the effective plastic strain. This concept is expressed mathematically in the equation shown below

$$\dot{W}^p = \sigma : \dot{\varepsilon}^p = \sigma : \dot{\lambda}\frac{\partial h}{\partial \sigma} = h\dot{\lambda} = \sigma_e \dot{\varepsilon}_e^p \tag{8}$$

where σ_e is the effective stress and ε_e^p is the effective plastic strain.

To compute the current value of the yield stresses needed for the yield function, the common practice in plasticity constitutive equations is to use analytical functions to define the evolution of the stresses as a function of the components of plastic strain (or the effective plastic strain). Alternatively, in the developed model tabulated stress-strain curves are used to track the yield stress evolution. The user is required to input twelve stress versus plastic strain curves. Specifically, the required curves include uniaxial tension curves in each of the normal directions (1,2,3), uniaxial compression curves in each of the normal directions (1,2,3), shear stress-strain curves in each of the shear directions (1-2, 2-3 and 3-1), and 45 degree off-axis tension curves in each of the 1-2, 2-3 and 3-1 planes. The 45 degree curves are required in order to properly capture the stress interaction effects. By utilizing tabulated stress-strain curves to track the evolution of the deformation response, the experimental stress-strain response of the material can be captured exactly without any curve fit approximations.

The required stress-strain data can be obtained either from actual experimental test results or by appropriate numerical experiments utilizing stand-alone codes. Currently, only static test data is considered. Future efforts will involve adding strain rate and temperature dependent effects to the computations. For certain composite architectures, the number of stress-strain curves that need to be input can be simplified. For example, for unidirectional composites, the normal response in the 3 direction can be assumed to be identical to the normal response in the 2 direction due to the transverse isotropy of the material. Likewise, the shear response in the 1-3 direction can be assumed to be identical to the shear response in the 1-2 direction. Similarly, the 45 degree off-axis curve in the 1-3 plane can be assumed to be identical to the 45 degree off-axis curve in the 1-2 plane. Due to the transverse isotropy of a unidirectional composite, one can also demonstrate that for the case of a unidirectional composite the 45 degree off-axis curve in the 2-3 plane is approximately equal to the normal stress-strain curve in the 2 (or 3 direction). For other composite architectures with significant symmetry (such as two-dimensional plain or satin weave composites), a certain degree of simplification in the stress-strain data that is required to be input is also possible.

To track the evolution of the deformation response along each of the stress-strain curves, the effective plastic strain is chosen to be tracking parameter. Using the numerical procedure described briefly later in this paper and in more detail in a companion paper [12], the effective plastic strain is computed for each time/load step. The stresses for each of the tabulated input curves corresponding to the current value of the effective plastic strain are then used to compute the yield function coefficients. To enable this tracking, each of the input stress-strain curves needs to be converted into a plot of stress versus effective plastic strain. To enable this conversion, the principal of the equivalence of plastic work is used again to relate the

Copyright by LSTC/Hallquist

unidirectional plastic strain increment to the effective plastic strain increment. For example, for the case of unidirectional loading in the 1 direction the effective plastic strain increment (and integrated current total plastic strain) can be computed as follows

$$\begin{aligned}
&\sigma_{ij} d\varepsilon_{ij}^p = \sigma_e d\varepsilon_e^p = h d\varepsilon_e^p \\
&\sigma_{11} d\varepsilon_{11}^p = h d\varepsilon_e^p \\
&\sigma_{11} d\varepsilon_{11}^p = \sqrt{H_{11}}\sigma_{11} d\varepsilon_e^p \\
&d\varepsilon_e^p = \frac{\sigma_{11} d\varepsilon_{11}^p}{\sqrt{H_{11}}\sigma_{11}} \\
&\varepsilon_e^p = \int \frac{\sigma_{11} d\varepsilon_{11}^p}{\sqrt{H_{11}}\sigma_{11}}
\end{aligned} \tag{9}$$

where σ_{11} is the unidirectional stress in the loading direction, $d\varepsilon_{11}^p$ is the plastic strain increment in the loading direction and $d\varepsilon_e^p$ is the increment in effective plastic strain. Note that in a general case the increment in effective plastic strain can be computed as the incremental area under the stress-plastic strain curve divided by the current value of the effective stress. A graphical representation of process is shown below in Figure 1.

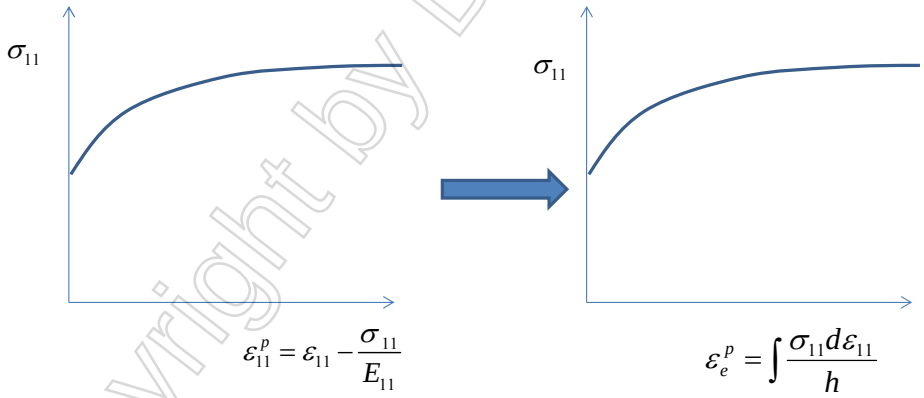

Figure 1: Conversion of stress versus plastic strain curves to stress versus effective plastic strain curves.

To compute the evolution of the effective plastic strain, a numerical algorithm based on the radial return method is employed. Given the revised value of the effective plastic strain, the yield stress values and the overall stress state of the material can be updated. Details of the numerical implementation are provided in a companion paper [12], but some of the key theoretical fundamentals of the algorithm are given below. The standard elastic constitutive equation is used to compute the revised stresses, where the flow law is applied for the computation of the plastic strains.

Copyright by DYNAmore

$$\dot{\sigma} = C:\left(\dot{\varepsilon} - \dot{\varepsilon}^{p}\right) = C:\left(\dot{\varepsilon} - \dot{\lambda}\frac{\partial h}{\partial \sigma}\right) \tag{10}$$

In the above equation, C is the standard elastic stiffness matrix, ε is the total strain, and the remainder of the terms are as defined previously. To compute the effective plastic strain rate, the consistency condition is applied in combination with the elastic constitutive equation

$$\begin{aligned}
\dot{f} &= \frac{\partial f}{\partial \sigma}\dot{\sigma} + \frac{\partial f}{\partial q}\dot{q} = 0 \\
\dot{f} &= \frac{\partial f}{\partial \sigma}\left(C:\dot{\varepsilon} - C:\dot{\lambda}\frac{\partial h}{\partial \sigma}\right) + \frac{\partial f}{\partial q}\dot{\lambda}\frac{dq}{d\lambda} = 0 \\
\dot{\lambda} &= \frac{\frac{\partial f}{\partial \sigma}C:\dot{\varepsilon}}{\frac{\partial f}{\partial \sigma}C:\frac{\partial h}{\partial \sigma} + \frac{\partial f}{\partial q}\frac{dq}{d\lambda}}
\end{aligned} \tag{11}$$

where f is the yield function defined in Equation (1) and q is the vector of yield stresses based on the input stress-strain curves.

$$q = \left(\sigma_{11}^{T} \quad \sigma_{22}^{T} \quad \sigma_{33}^{T} \quad \sigma_{11}^{C} \quad \sigma_{22}^{C} \quad \sigma_{33}^{C} \quad \sigma_{12} \quad \sigma_{23} \quad \sigma_{31} \quad \sigma_{12}^{45} \quad \sigma_{23}^{45} \quad \sigma_{31}^{45}\right) \tag{12}$$

To compute the derivative of the q vector with respect to the effective plastic strain λ, a chain rule type of computation is carried out.

$$\frac{dq}{d\lambda} = \frac{dq}{d\varepsilon^{p}}\frac{d\varepsilon^{p}}{d\lambda} \tag{13}$$

The derivative of the yield stress vector with respect to plastic strain is the instantaneous slope of the stress versus plastic strain curve from each of the 12 input stress-strain curves. The derivative of the plastic strain with respect to the plastic multiplier λ can be computed from the flow law for each of the specialized unidirectional (or off-axis) cases represented by the input stress-strain curves. Note that for the off-axis cases the flow law must first be written in the material axis system and then the plastic strains must be transformed into the structural axis system in order to compute the proper derivative of the plastic strain with respect to the plastic multiplier. A secant iteration approach is used in combination with the radial return method to compute the specific value of the effective plastic strain rate [12].

Characterization of Flow Law Coefficients

The coefficients in the flow rule need to be characterized based on data obtained from experimental stress-strain curves for the composite. Specifically, data from the 12 experiments leading to the input stress-strain curves must be utilized. The data can be obtained either from actual experiments or numerical experiments. For example, if one knows the mechanical

Copyright by DYNAmore

properties and stress-strain curves for the fiber and matrix constituents, numerical analyses can be conducted using either high fidelity finite element analysis (where the fiber and matrix are modeled as distinct constituents) or analytical tools such as the NASA Glenn developed micromechanics code MAC/GMC [14] to obtain numerical approximations to the actual composite experimental data.

First, the procedures used to obtain the required coefficients for the simplified case of a unidirectional carbon fiber based polymer matrix composite will be discussed. Afterward, a generalized procedure to obtain the required constants for a general composite will be presented. For a unidirectional carbon fiber composite, as discussed by Sun and Chen [11] a reasonable approximation to make is that due to the linear behavior of the carbon fiber the plastic strain in the fiber direction (the 1 direction) is equal to zero for all values of stress. By examining the second expression in Equation (6), one can conclude that for a general stress state the only way the plastic strain in the 1 direction can be zero is for the coefficients H_{11}, H_{12} and H_{13} to all be identically zero. Next, since the transverse tension response of the composite can display a certain degree of nonlinearity, a reasonable approximation to make is that for the case of a unidirectional load in the 2 direction the effective stress is equal to the applied transverse tension stress σ_{22}. By simplifying the plastic potential function g (shown in Equation (5)) for the case of a unidirectional transverse tension stress, and by setting this term (along with the transverse tensile stress) equal to the effective stress, one can show that the value of the coefficient H_{22} must equal one. Since a unidirectional composite is transversely isotropic, one can set the value of H_{33} to also equal one. Given these values, using the definition of the plastic Poisson's ratio υ_{23} shown in Equation (7), one can find that the coefficient H_{23} equals the negative of the plastic Poisson's ratio υ_{23}. Since the flow surface coefficients are assumed to be constant, an average value of the plastic Poisson's ratio must be determined from the experimental and/or numerical test data from a unidirectional transverse tension test. To determine the in-plane shear coefficient H_{44}, utilizing a procedure similar to that developed by Sun and Chen [11] for their model, the plastic potential function g given in Equation (5) and the plastic strain definition given in Equation (6) can be simplified for the case of in-plane shear loading in the 12 direction, yielding the following expressions.

$$g = \sigma_e = \sigma_{12}\sqrt{H_{44}}$$
$$\varepsilon_{12}^p = 0.5\varepsilon_e^p\sqrt{H_{44}} \Rightarrow \varepsilon_e^p = \frac{\varepsilon_{12}^p}{0.5\sqrt{H_{44}}} \tag{14}$$

Starting from the experimental stress versus plastic strain plot for the case of in-plane shear loading, using the expressions in Equation (14) the value of H_{44} can be optimized to provide the closest possible match with the overall effective stress versus effective strain curve, selected for the case of a unidirectional carbon fiber composite to be the transverse tension stress versus plastic strain curve. Due to the transverse isotropy of the unidirectional composite, the value of the coefficient H_{66} can be set equal to the value of the coefficient H_{44}. To determine the value of the H_{55} coefficient, a similar procedure can be carried out for the case of shear loading in the 23 direction. Alternatively, due to the transverse isotropy of the composite, by computing the effective stress for the case of off-axis loading in the 2-3 plane, an isotropic type of relation can be determined for the coefficient H_{23}

Copyright by DYNAmore

$$H_{55} = 2\left(1 + \nu_{23}^{p}\right) \tag{15}$$

where υ_{23}^{p} is the plastic Poisson's ratio in the 23 direction, obtained from the material data.

Similar procedures are used for the case of a general composite with no identified symmetries. An example of a general composite would be a triaxially braided composite which is modeled as a smeared, homogenous material. Another example would be a generalized laminated composite modeled as a smeared, homogeneous material. For the case of a general composite, a unidirectional tension test in the longitudinal (1) direction is chosen as the baseline case. By utilizing Equation (5) and setting the plastic potential function and the unidirectional longitudinal stress equal to the effective stress, the value of the H_{11} coefficient can be found to equal one. Based on the relations given in Equation (7), the value of the coefficient H_{12} can be found to equal the negative of the plastic Poisson's ratio ν_{12}^{p}, and the value of the coefficient H_{13} can be found to be equal to the negative of the plastic Poisson's ratio ν_{13}^{p}. As before, the value of the plastic Poisson's ratio used in the computations is the average value of the parameter determined from the experimental and/or numerically obtained data. In a similar fashion, the values of the coefficients H_{22}, H_{23} and H_{33} can be computed.

$$\begin{aligned} H_{22} &= \frac{\nu_{12}^{p}}{\nu_{21}^{p}} \\ H_{23} &= -\nu_{23}^{p}\,\frac{\nu_{12}^{p}}{\nu_{21}^{p}} \\ H_{33} &= \frac{\nu_{13}^{p}}{\nu_{31}^{p}} \end{aligned} \tag{16}$$

To compute the values of the coefficients H_{44}, H_{55}, and H_{66}, the same procedure that was utilized to compute G_{44} for the case of a unidirectional carbon fiber composite is used, only all three shear loading cases (σ_{12}, σ_{23}, and σ_{31}) must be used.

Conclusions

A generalized plasticity model suitable for use in polymer composite impact simulations has been developed. The plasticity model will be part of a generalized plasticity and damage model which will be implemented into LS-DYNA as MAT_213. The yield function is based on the Tsai-Wu composite failure model, and a suitable nonassociative flow rule was defined. Methods of utilizing tabulated stress-strain data to track the evolution of the yield stresses as a function of the effective plastic strain have been developed. The elastic constitutive equation can be used in combination with the consistency condition to compute the effective plastic strain. In a companion paper [12], further details of the numerical algorithm are provided along with examples of verification and validation studies which have been performed to examine the accuracy and efficiency of the analytical model.

Future efforts will involve the development of an equivalent damage model, to be employed in combination with the plasticity model, which will also be based on utilizing tabulated stress-strain data to track the evolution of damage in the composite. Element failure will also be

Copyright by DYNAmore

incorporated within the model. In addition, strain rate and temperature effects will be added to the analysis capability. Overall, when completed the composite model as implemented in MAT_213 will provide significant improvements to the state of the art in the modeling of the impact response of polymer matrix composites.

Acknowledgements

Authors Hoffarth, Harrington and Rajan gratefully acknowledge the support of the Federal Aviation Administration through Grant #12-G-001 entitled "Composite Material Model for Impact Analysis", William Emmerling, Technical Monitor.

References

[1] Hallquist, J.: LS-DYNA Keyword User's Manual, Version 970. Livermore Software Technology Corporation, Livermore, CA, 2013.
[2] Chang, F.-K.; and Chang, K.-Y.: "A Progressive Damage Model for Laminated Composites Containing Stress Concentrations," *Journal of Composite Materials*, Vol. 21, pp. 834-855, 1987.
[3] Matzenmiller, A.; Lubliner, J; and Taylor, R.L.: "A constitutive model for anisotropic damage in fiber-composites," *Mechanics of Materials*, Vol. 20, pp. 125-152, 1995.
[4] Yen, C.F.: ""Ballistic Impact Modeling of Composite Materials," 7th International LS-DYNA Users Conference, Livermore Software Technology Corporation, 2002.
[5] Williams, K.V.; Vaziri, R.; and Poursartip, A.: "A physically based continuum damage mechanics model for thin laminated composite structures," *International Journal of Solids and Structures*, Vol. 40, pp. 2267-2300, 2003.
[6] Pinho, S.T.; Iannucci, L.; and Robinson, P.: "Physically-based failure models and criteria for laminated fibre-reinforced composites with emphasis on fibre kinking: Part I: Development," *Composites: Part A*, Vol. 37, pp. 63–73, 2006.
[7] Pinho, S.T.; Iannucci, L.; and Robinson, P.: "Physically-based failure models and criteria for laminated fibre-reinforced composites with emphasis on fibre kinking: Part II: FE implementation," *Composites: Part A*, Vol. 37, pp. 766–777, 2006.
[8] Maimi, P.; Camanho, P.P.; Mayugo, J.A.; and Davila, C.G.: "A continuum damage model for composite laminates: Part I – Constitutive model," *Mechanics of Materials*, Vol. 39, pp. 897–908, 2007.
[9] Maimi, P.; Camanho, P.P.; Mayugo, J.A.; and Davila, C.G.: "A continuum damage model for composite laminates: Part II – Computational implementation and validation," *Mechanics of Materials*, Vol. 39, pp. 909-919, 2007.
[10] Daniel, I.M; and Ishai, O.: Engineering Mechanics of Composite Materials. Oxford University Press, New York, 2006.
[11] Sun, C.T.; and Chen, J.L.: "A Simple Flow Rule for Characterizing Nonlinear Behavior of Fiber Composites," *Journal of Composite Materials*, Vol. 23, pp. 1009-1020, 1989.
[12] Hoffarth, C.; Harrington, J.; Rajan, S.; Goldberg, R.; Carney, K.; DuBois, P.; Blankenhorn, G.: "Verification and Validation of a Three-Dimensional Generalized Composite Material Model," 13th International LS-DYNA Users Conference, Livermore Software Technology Corporation, 2014.
[13] Khan, A.S.; and Huang, S.: Continuum Theory of Plasticity. John Wiley and Sons, New York, 1995.
[14] Bednarcyk, B.A.; and Arnold, S.M.: 2002. "MAC/GMC 4.0 User's Manual - Keywords Manual," NASA/TM-2002-212077/VOL2, National Aeronautics and Space Administration, Washington, D.C., 2002.

Copyright by DYNAmore